Tropomodulin1 as a potential contributor to metastasis in human oral cancer

（ヒト口腔癌の転移における潜在的寄与要因としての *Tropomodulin1* について）

千葉大学大学院医学薬学府

先端医学薬学専攻

（主任:　丹沢　秀樹　教授）

鈴木　寿和

Abstract

Tropomodulin1 (TMOD1), which regulates the length and depolymerization of actin filaments by binding to the pointed end of the actin filament, has been reported to be a powerful diagnostic marker for ALK-negative anaplastic large-cell lymphoma; however, little is known about the relevance of TMOD1 in the behaviors of oral squamous cell carcinoma (OSCC). We evaluated TMOD1 expression in OSCC-derived cell lines and primary OSCC samples (n=200) using quantitative reverse transcriptase-polymerase chain reaction, immunoblotting, and semiquantitative immunohistochemistry. We also analyzed the clinical correlation between TMOD1 expression status and clinical parameters in patients with OSCC and performed a prospective study using 40 primary OSCC samples. TMOD1 expression was up-regulated significantly ($p<0.05$) in OSCC *in vitro* and *in vivo* compared with normal counterparts. TMOD1 expression also was correlated significantly ($p=0.0199$ and $p=0.0064$, respectively) with regional lymph node metastasis (RLNM) and 5-year survival rates. This prospective study also showed that high TMOD1 expression was seen in 12 (75%) of 16 cases in RLNM-positive patients and nine (37.5%) of 24 cases in RLNM-negative patients. The current data provided the first evidence that TMOD1 expression is a critical biomarker for RLNM and prognosis of patients with OSCC.

Introduction

Oral squamous cell carcinoma (OSCC) is a frequently occurring neoplasm that is usually aggressive and has a poor prognosis (1). OSCC accounts for more than 50% of all head and neck SCC. The prognosis in advanced cases is poor, and 5-year survival rates of OSCC are below 50% (2,3). The 5-year survival rate is 90% for patients without metastasis but less than 40% for patients with metastasis, suggesting that regional lymph node metastasis (RLNM) is one of the most adverse prognostic factors (4-10). However, the mechanisms of metastasis are poorly understood (11). Therefore, molecular changes in a number of oncogenes and tumor suppressor genes associated with development of OSCC may be important clues for preventing this disease, and elucidating the molecular mechanisms involved in cancer metastasis is needed (3,4).

The tropomodulin family (TMOD1-4) is expressed differentially in a tissue-specific manner and is involved in regulating actin filament architecture in diverse cellular types (12). TMOD1-4 are 70% similar in amino acid sequence with different expression profiles (13) and contain an N-terminal unstructured domain and a C-terminal domain consisting of 5 leucine-rich repeat motifs (14,15). TMOD1-4 inhibit elongation and depolymerization of actin filaments by binding to the pointed end of the actin filament (16-18). Among them, TMOD1 has two actin-binding regions and two tropomyosin-binding regions (19-22).

Recent studies have reported that TMOD1 is a diagnostic marker for triple-negative breast cancers and ALK-negative anaplastic large-cell lymphoma (23,24); however, the role of TMOD1 in OSCC remains unknown. We present the results of measurements of TMOD1 levels in OSCC that are clinically and functionally linked to RLNM.

Materials and methods

Ethics statement. The Ethical Committee of the Graduate School of Medicine, Chiba University (approval number, 236) approved the study protocol, which was performed in accordance with the tenets of the Declaration of Helsinki. All patients provided written informed consent.

OSCC-derived cell lines and tissue specimens. Human OSCC-derived cell lines (HSC-2, HSC-3, HSC-4, Sa3, Ca9-22, Ho-1-u-1, Ho-1-N-1, KOSC-2, and SAS) were obtained from the Human Science Research Resources Bank (Osaka, Japan) or the RIKEN BioResource Center (Ibaraki, Japan) through the National BioResource Project of the Ministry of Education, Culture, Sports, Science and Technology in Japan. Primary cultured human normal oral keratinocytes (HNOKs) were obtained from healthy oral mucosal epithelial specimens collected from young patients at Chiba University Hospital (25-28). All cells were grown in Dulbecco's modified Eagle medium (Sigma-Aldrich, St. Louis, MO, USA) supplemented with 10% fetal bovine serum (Sigma-Aldrich) and 50 units/ml of penicillin and streptomycin (Sigma-Aldrich).

Two hundred primary OSCC specimens and patient-matched normal epithelial specimens were obtained during surgeries performed at Chiba University Hospital (Table 1). The resected tissues were fixed in 20% buffered formaldehyde solution for pathologic diagnosis and immunohistochemical (IHC) staining. We performed histopathological diagnosis of each OSCC sample according to the World Health Organization criteria at the Department of Pathology of Chiba University Hospital (29). The clinicopathological stages

were determined based on the TNM classification of the International Union against Cancer (30).

mRNA expression analysis. Total RNA was isolated using Trizol Reagent (Invitrogen, Carlsbad, CA, USA), according to the manufacturer's instructions. cDNA was generated using ReverTra Ace qPCR RT Master Mix (Toyobo Life Science, Osaka, Japan) according to the manufacturer's instructions. Real-time quantitative reverse transcriptase-polymerase chain reaction (qRT-PCR) was performed in a 20-μl reaction volume using the LightCycler 480 apparatus (Roche Diagnostics, Mannheim, Germany), according to the manufacturer's protocol. The general amplification conditions were performed as described previously (31-33). Primers and universal probes were designed using the Universal Probe Library Assay Design Center (Roche Diagnostics), which specifies the most suitable set. The primer sequences used for qRT-PCR were: *TMOD1*, forward, 5′-AGCTGAGGACCCTGGAAAAT-3′; reverse, 5′- GCAGGCAGCAGTGCATTAT-3′; and universal probe #42, and the *glyceraldehyde-3-phosphate dehydrogenase* (*GAPDH*), forward, 5′-CATCTCTGCCCCCTCTGCTGA-3′; reverse, 5′-GGATGACCTTGCCCACAGCCT-3′; and universal probe #60. The transcript amount for TMOD1 was estimated from the respective standard curves and normalized to the *GAPDH* transcript amount determined in corresponding samples.

Immunoblotting analysis. The cells were washed three times with cold phosphate buffered saline (PBS) and gently and briefly centrifuged. The cellular pellets were incubated at 4°C for

30 minutes in a lysis buffer (7 M urea, 2 M thiourea, 4% w/v CHAPS, and 10 mM Tris; pH 7.4) with a proteinase inhibitor cocktail (Roche Diagnostics). The total protein concentration was measured using a dye-binding method based on the Bradford assay with Bio-Rad Protein Assay Dye Reagent Concentrate (Bio-Rad Laboratories, Hercules, CA, USA).

Protein extracts were electrophoresed on 4-12% Bis-Tris gel and transferred to nitrocellulose membranes (Invitrogen) and blocked for 1 hour at room temperature with Blocking One (Nacalai Tesque, Inc., Kyoto, Japan). The membranes were washed three times with 0.1% Tween-20 in Tris-buffered saline (TBS-T) and incubated with affinity-purified rabbit anti-TMOD1 monoclonal antibody (Santa Cruz Biotechnology, Santa Cruz, CA, USA) and mouse anti-GAPDH monoclonal antibody overnight at 4°C. The membrane was washed with TBS-T and incubated with horseradish peroxidase-conjugated anti-rabbit or anti-mouse IgG as a secondary antibody (Promega, Madison, WI, USA), for 1 hour at room temperature. Finally, the membranes were detected using Super-Signal West Pico Chemiluminescent substrate (Thermo Fisher Scientific, Rockford, IL, USA), and immunoblotting was visualized by exposing the membranes to the ChemiDoc XRS Plus System (Bio-Rad Laboratories). The signal intensities were quantitated using the Image Lab system (Bio-Rad Laboratories). Densitometric TMOD1 protein data were normalized to GAPDH protein levels.

Semiquantitative IHC. Semiquantitative IHC (sq-IHC) of 4-μm sections of paraffin-embedded OSCC clinical specimens was performed. Briefly, after paraffinization, hydration, activation of antigen, hydrogen peroxide quenching, and blocking, the clinical sections were incubated with rabbit anti-TMOD1 monoclonal antibody (Santa Cruz

Biotechnology) at 4°C in a moist chamber overnight. Upon incubation with the primary antibody, the specimens were washed three times with PBS and treated with Envision reagent (DAKO, Carpinteria, CA, USA) followed by color development in 3,3'-diaminobenzidine tetrahydrochloride (DAKO). The slides then were counterstained lightly with hematoxylin, dehydrated with ethanol, cleaned with xylene, and mounted. To quantify the status of the TMOD1 protein expression in clinical samples, we used the sq-IHC scoring systems described previously (28,34-38). The mean percentages of positive tumoral cells were determined in at least three random fields in each section; the intensities of the TMOD1-immunoreactions were scored as follows: 0+, none; 1+, weak; 2+, moderate; and 3+, intense. The staining intensity and the cellular numbers were multiplied to produce a TMOD1 sq-IHC score. To determine the cutoff points of the TMOD1 sq-IHC scores, we analyzed the OSCCs sq-IHC scores of 200 patients using receiver operating characteristic (ROC) curves. Two independent pathologists from Chiba University Hospital, neither of whom had knowledge of the patients' clinical status, made these judgments. To calculate the 5-year survival rate, we surveyed each patient's life and month of death.

Prospective study. To evaluate the effect of the cutoff value from RLNM by ROC curve analysis, we performed a prospective study using 40 primary OSCC specimens at Chiba University Hospital. We randomly selected 40 primary OSCC specimens and analyzed the correlation between RLNM and TMOD1 expression using sq-IHC.

Statistical analysis. To compare the TMOD1 expression levels, statistical significance was

evaluated using the Mann-Whitney *U*-test. The relationships between the TMOD1 sq-IHC scores and clinicopathological profiles were evaluated using the Student's *t*-test and the Mann-Whitney *U*-test. The 5-year survival rate was evaluated using the log-rank test. $P<0.05$ was considered statistically significant. The data are expressed as the mean ± the standard error of the mean.

Results

Up-regulation of TMOD1 in OSCC-derived cell lines. To investigate the expression status of TMOD1, we performed qRT-PCR and immunoblotting analyses using nine OSCC-derived cell lines (HSC-2, HSC-3, HSC-4, Sa3, Ca9-22, Ho-1-u-1, Ho-1-N-1, KOSC-2, and SAS) and HNOKs. *TMOD1* mRNA was up-regulated significantly ($p<0.05$) in all OSCC-derived cell lines compared with the HNOKs (Fig. 1A). We also performed immunoblotting analysis to investigate the TMOD1 protein expression in the OSCC-derived cell lines and the HNOKs (Fig. 1B). A significant increase in TMOD1 protein expression was seen in all OSCC-derived cell lines compared with the HNOKs.

Evaluation of TMOD1 expression in primary OSCCs. To investigate the expression status of TMOD1 in primary OSCCs and the relation to the clinicopathological characteristics, we analyzed the TMOD1 protein expression in primary OSCC specimens from 200 patients (Table 1) using the sq-IHC scoring system. We showed representative IHC results for TMOD1 protein in primary OSCCs (Fig. 2A) and normal oral tissue (Fig. 2B). Strong TMOD1 immunoreactivity was detected in the cytoplasm of primary OSCCs; however, normal oral tissue showed almost negative immunostaining. The TMOD1 protein expression of primary OSCCs was significantly ($p<0.05$) higher than in normal tissue (Fig. 2C). The TMOD1 sq-IHC scores in OSCCs and adjacent normal oral tissues ranged from 204.44 to 7.00 (median, 100.00) and 105.50 to 4.00 (median, 35.83), respectively.

Evaluation of TMOD1 expression in primary OSCCs by age at surgery, gender, primary tumoral size, histologic type, and vascular invasiveness. We did not find differences between TMOD1 protein expression and these clinical parameters (Fig. 3A-E) (age at surgery, p=0.181; gender, p=0.417; primary tumoral size, p=0.057; histologic type, p=0.073; or vascular invasion, p=0.558).

Evaluation of TMOD1 expression in primary OSCCs by RLNM. The ROC curve analysis showed that the area under the curve (AUC) was 0.608 (95% confidence interval [CI], 0.527-0.688; sensitivity, 65.8%; specificity, 57.5%) and the cutoff value was 100.00 (Fig. 4A). The TMOD1 sq-IHC scores of the RLNM-negative patients and RLNM-positive patients ranged from 204.44 to 12.50 (median, 85.48) and 201.17 to 7.00 (median, 112.16), respectively. TMOD1 protein expression of primary OSCCs with RLNM was significantly (p=0.0199) higher than without RLNM (Fig. 4B).

Evaluation of TMOD1 expression in primary OSCCs with 5-year survival. Using the cutoff value from RLNM from ROC curve analysis, the 5-year survival rates in the TMOD1-positive OSCCs (n=103) and the TMOD1-negative OSCCs (n=97) were 60.4% and 79.9%, respectively. The survival rates in the TMOD1-positive group were significantly (p=0.0064) lower than those in the TMOD1-negative group (Fig. 5).

Prospective study of TMOD1 expression in primary OSCCs. To determine if the cutoff value of the TMOD1 IHC scores from RLNM (Fig. 4) are useful as a clinical indicator, we

prospectively assessed the correlation between RLNM and TMOD1 expression in 40 patients with OSCC. High TMOD1 expression was seen in 12 (75%) of 16 RLNM-positive patients and nine (37.5%) of 24 RLNM-negative patients. Thus, TMOD1 expression was significantly ($p=0.027$) higher in the RLNM-positive patients (Table 2).

Discussion

We found that TMOD1 was overexpressed frequently in OSCC *in vitro* and *in vivo* ($p<0.05$; Figs. 1, 2), and that TMOD1 expression in RLNM-positive patients with OSCC was significantly ($p<0.05$) greater than in RLNM-negative patients (Fig. 4). In addition, the survival rates in the TMOD1-positive patients were significantly lower than in the TMOD1-negative patients (Fig. 5). In the prospective study, high TMOD1 expression was seen in 12 (75%) of 16 RLNM-positive patients and nine (37.5%) of 24 RLNM-negative patients (Table 2).

OSCCs are characterized by a high degree of local invasiveness and a high rate of RLNM in an early phase (39). A study reported recently that 37% of patients with OSCC had RLNM (40). The 5-year survival rate in RLNM-negative patients was 81%, whereas that in RLNM-positive patients was 57% (40). Metastasis represents a highly organized, non-random, organ-specific, and multistep process (41). Although many molecules, such as integrins and matrix metalloproteinases (MMPs), play key roles in cancer cell invasiveness and metastasis (42-44), the precise factors and mechanisms affecting its preferred migration and invasion into the regional lymph nodes are poorly understood. Overexpression of TMOD1, a novel target of NF-κB, induces the translocation of β-catenin to nucleus, leading to activation of MMPs in triple-negative breast cancer samples (23). Since NF-κB signaling also relates to RLNM and tumor-induced lymphangiogenesis (45), TMOD1 may contribute to the cellular invasiveness and metastasis in OSCCs.

In conclusion, the current results indicated that TMOD1 is overexpressed frequently in human oral cancer. TMOD1 overexpression is associated with RLNM and the 5-year

survival rate. The prospective study also confirmed the correlation between TMOD1 expression and RLNM. While further studies are needed to study the NF-κB–TMOD1 axis in the cancer microenvironment, TMOD1 overexpression may directly affect tumoral metastasis in OSCCs, and TMOD1 may be a critical biomarker of RLNM and a therapeutic target to prevent metastasis in OSCCs.

Acknowledgments

We thank Lynda C. Charters for editing this manuscript. The authors received no financial support.

References

1. Severino P, Alvares AM, Michaluart P, Jr., et al.: Global gene expression profiling of oral cavity cancers suggests molecular heterogeneity within anatomic subsites. BMC Res Notes 1: 113, 2008.
2. Yao M, Epstein JB, Modi BJ, Pytynia KB, Mundt AJ and Feldman LE: Current surgical treatment of squamous cell carcinoma of the head and neck. Oral Oncol 43: 213-223, 2007.
3. Casiglia J and Woo S: A comprehensive review of oral cancer. General dentistry 49: 72-82, 2000.
4. Takes RP: Staging of the neck in patients with head and neck squamous cell cancer: imaging techniques and biomarkers. Oral Oncol 40: 656-667, 2004.
5. Karatzanis AD, Waldfahrer F, Psychogios G, et al.: Resection margins and other prognostic factors regarding surgically treated glottic carcinomas. J Surg Oncol 101: 131-136, 2010.
6. Fan S, Tang QL, Lin YJ, et al.: A review of clinical and histological parameters associated with contralateral neck metastases in oral squamous cell carcinoma. Int J Oral Sci 3: 180-191, 2011.
7. Lea J, Bachar G, Sawka AM, et al.: Metastases to level IIb in squamous cell carcinoma of the oral cavity: a systematic review and meta-analysis. Head Neck 32: 184-190, 2010.
8. Okura M, Aikawa T, Sawai NY, Iida S and Kogo M: Decision analysis and treatment threshold in a management for the N0 neck of the oral cavity carcinoma. Oral Oncol 45: 908-911, 2009.
9. Greenberg JS, Fowler R, Gomez J, et al.: Extent of extracapsular spread: a critical prognosticator in oral tongue cancer. Cancer 97: 1464-1470, 2003.
10. Sano D and Myers JN: Metastasis of squamous cell carcinoma of the oral tongue. Cancer Metastasis Rev 26: 645-662, 2007.
11. Tanaka J, Irie T, Yamamoto G, et al.: ANGPTL4 regulates the metastatic potential of oral squamous cell carcinoma. J Oral Pathol Med 44: 126-133, 2015.
12. Lewis RA, Yamashiro S, Gokhin DS and Fowler VM: Functional effects of mutations in the tropomyosin-binding sites of tropomodulin1 and tropomodulin3. Cytoskeleton (Hoboken) 71: 395-411, 2014.
13. Bliss KT, Tsukada T, Novak SM, et al.: Phosphorylation of tropomodulin1 contributes to the regulation of actin filament architecture in cardiac muscle. FASEB J 28: 3987-3995,

2014.
14. Krieger I, Kostyukova A, Yamashita A, Nitanai Y and Maéda Y: Crystal structure of the C-terminal half of tropomodulin and structural basis of actin filament pointed-end capping. Biophysical journal 83: 2716-2725, 2002.
15. Kostyukova A, Maeda K, Yamauchi E, Krieger I and Maéda Y: Domain structure of tropomodulin. European Journal of Biochemistry 267: 6470-6475, 2000.
16. Kostyukova A: Tropomodulins and tropomodulin/tropomyosin interactions. Cellular and molecular life sciences 65: 563-569, 2008.
17. Gregorio CC, Weber A, Bondad M, Pennise CR and Fowler VM: Requirement of pointed-end capping by tropomodulin to maintain actin filament length in embryonic chick cardiac myocytes. Nature 377: 83-86, 1995.
18. Tsukada T, Kotlyanskaya L, Huynh R, et al.: Identification of residues within tropomodulin-1 responsible for its localization at the pointed ends of the actin filaments in cardiac myocytes. J Biol Chem 286: 2194-2204, 2011.
19. Fowler VM, Greenfield NJ and Moyer J: Tropomodulin contains two actin filament pointed end-capping domains. J Biol Chem 278: 40000-40009, 2003.
20. Greenfield NJ, Kostyukova AS and Hitchcock-DeGregori SE: Structure and tropomyosin binding properties of the N-terminal capping domain of tropomodulin 1. Biophysical journal 88: 372-383, 2005.
21. Kostyukova AS, Choy A and Rapp BA: Tropomodulin binds two tropomyosins: a novel model for actin filament capping. Biochemistry 45: 12068-12075, 2006.
22. Kostyukova AS, Rapp BA, Choy A, Greenfield NJ and Hitchcock-DeGregori SE: Structural requirements of tropomodulin for tropomyosin binding and actin filament capping. Biochemistry 44: 4905-4910, 2005.
23. Ito-Kureha T, Koshikawa N, Yamamoto M, et al.: Tropomodulin 1 expression driven by NF-kappaB enhances breast cancer growth. Cancer Res 75: 62-72, 2015.
24. Agnelli L, Mereu E, Pellegrino E, et al.: Identification of a 3-gene model as a powerful diagnostic tool for the recognition of ALK-negative anaplastic large-cell lymphoma. Blood 120: 1274-1281, 2012.
25. Kasamatsu A, Uzawa K, Nakashima D, et al.: Galectin-9 as a regulator of cellular adhesion in human oral squamous cell carcinoma cell lines. Int J Mol Med 16: 269-273, 2005.
26. Endo Y, Uzawa K, Mochida Y, et al.: Sarcoendoplasmic reticulum Ca(2+) ATPase type 2

downregulated in human oral squamous cell carcinoma. Int J Cancer 110: 225-231, 2004.
27. Sakuma K, Kasamatsu A, Yamatoji M, et al.: Expression status of Zic family member 2 as a prognostic marker for oral squamous cell carcinoma. J Cancer Res Clin Oncol 136: 553-559, 2010.
28. Yamatoji M, Kasamatsu A, Kouzu Y, et al.: Dermatopontin: a potential predictor for metastasis of human oral cancer. Int J Cancer 130: 2903-2911, 2012.
29. Pindborg J, Reichart P, Smith C and Van der Waal I: Histological Typing of Cancer and Precancer of the Oral Mucosa Springer. Berlin Heidelberg, 1997.
30. Sobin LH, Gospodarowicz MK and Wittekind C: TNM classification of malignant tumours. John Wiley & Sons, 2011.
31. Shimizu F, Shiiba M, Ogawara K, et al.: Overexpression of LIM and SH3 Protein 1 leading to accelerated G2/M phase transition contributes to enhanced tumourigenesis in oral cancer. PLoS One 8: e83187, 2013.
32. Iyoda M, Kasamatsu A, Ishigami T, et al.: Epithelial cell transforming sequence 2 in human oral cancer. PLoS One 5: e14082, 2010.
33. Baba T, Sakamoto Y, Kasamatsu A, et al.: Persephin: A potential key component in human oral cancer progression through the RET receptor tyrosine kinase-mitogen-activated protein kinase signaling pathway. Mol Carcinog, 2013.
34. Minakawa Y, Kasamatsu A, Koike H, et al.: Kinesin family member 4A: a potential predictor for progression of human oral cancer. PLoS One 8: e85951, 2013.
35. Lombardi DP, Geradts J, Foley JF, Chiao C, Lamb PW and Barrett JC: Loss of KAI1 Expression in the Progression of Colorectal Cancer. Cancer Research 59: 5724-5731, 1999.
36. Lombardi DP, Geradts J, Foley JF, Chiao C, Lamb PW and Barrett JC: Loss of KAI1 expression in the progression of colorectal cancer. Cancer Res 59: 5724-5731, 1999.
37. Shimada K, Uzawa K, Kato M, et al.: Aberrant expression of RAB1A in human tongue cancer. Br J Cancer 92: 1915-1921, 2005.
38. Kouzu Y, Uzawa K, Koike H, et al.: Overexpression of stathmin in oral squamous-cell carcinoma: correlation with tumour progression and poor prognosis. Br J Cancer 94: 717-723, 2006.
39. Maula S-M, Luukkaa M, Grénman R, Jackson D, Jalkanen S and Ristamäki R: Intratumoral lymphatics are essential for the metastatic spread and prognosis in

squamous cell carcinomas of the head and neck region. Cancer research 63: 1920-1926, 2003.

40. Kim SY, Nam SY, Choi SH, Cho KJ and Roh JL: Prognostic value of lymph node density in node-positive patients with oral squamous cell carcinoma. Ann Surg Oncol 18: 2310-2317, 2011.
41. Nicolson GL: Paracrine and autocrine growth mechanisms in tumor metastasis to specific sites with particular emphasis on brain and lung metastasis. Cancer and Metastasis Reviews 12: 325-343, 1993.
42. Thomas GJ, Lewis MP, Hart IR, Marshall JF and Speight PM: αvβ6integrin promotes invasion of squamous carcinoma cells through up‐regulation of matrix metalloproteinase‐9. International journal of cancer 92: 641-650, 2001.
43. Ylipalosaari M, Thomas G, Nystrom M, et al.: αvβ6 integrin down-regulates the MMP-13 expression in oral squamous cell carcinoma cells. Experimental cell research 309: 273-283, 2005.
44. Ramos DM, But M, Regezi J, et al.: Expression of integrin β6 enhances invasive behavior in oral squamous cell carcinoma. Matrix Biology 21: 297-307, 2002.
45. Su C, Chen Z, Luo H, et al.: Different patterns of NF-kappaB and Notch1 signaling contribute to tumor-induced lymphangiogenesis of esophageal squamous cell carcinoma. J Exp Clin Cancer Res 30: 85, 2011.

Legends

Figure 1. Up-regulation of TMOD1 in OSCC-derived cell lines. (A) Quantification of *TMOD1* mRNA expression in OSCC-derived cell lines by qRT-PCR analysis. Significant ($^{*}p<0.05$, Student's *t*-test) up-regulation of *TMOD1* mRNA is seen in nine OSCC-derived cell lines compared with the HNOKs. Data are expressed as the mean ± SEM of triplicate results (A). Immunoblotting analysis of TMOD1 protein in OSCC-derived cell lines. TMOD1 protein expression is up-regulated in OSCC-derived cell lines compared with that in the HNOKs. Densitometric TMOD1 protein data are normalized to the GAPDH protein levels. The values are expressed as percentages of the HNOKs (B).

Figure 2. Evaluation of TMOD1 expression in primary OSCCs. Representative sq-IHC results of TMOD1 in primary OSCCs (A) and normal oral tissues (B). Original magnification, ×200. The status of TMOD1 protein expression in primary OSCCs (n=200) and normal counterparts by the sq-IHC scoring system. The TMOD1 sq-IHC scores for OSCCs and normal oral tissues range from 204.44 to 7.00 (median, 100.00) and 105.50 to 4.00 (median, 35.83), respectively. TMOD1 protein expression levels in OSCCs are significantly (*$p<0.05$, Student's *t*-test) higher than in normal oral tissue (C).

Figure 3. Evaluation of TMOD1 expression in primary OSCCs by various clinical parameters. The evaluation of TMOD1 expression based on the age at surgery shows that the optimal cutoff point in the ROC curve analysis is 152.6 (AUC, 0.556; 95% CI,

0.476-0.636; sensitivity, 88.8%; specificity, 25.5%). The TMOD1 OSCCs sq-IHC scores in patients under 70 years of age and over 70 years of age range from 204.44 to 24.00 (median, 103.00) and 200.00 to 7.00 (median, 94.00), respectively. The TMOD1 protein expression in the primary OSCCs does not differ significantly (p=0.18, Student's *t*-test) between the two age groups (A). Evaluation of TMOD1 expression in primary OSCCs by gender shows that the optimal cutoff point in the ROC curve analysis is 104.0 (AUC, 0.530; 95% CI, 0.445-0.616; sensitivity, 47.7%; specificity, 61.2%). The TMOD1 OSCCs sq-IHC scores in males and females range from 201.17 to 7.00 (median, 101.00) and 204.44 to 12.50 (median, 89.92), respectively. The TMOD1 protein expression in the primary OSCCs does not differ significantly (p=0.417, Student's *t*-test) between males and females (B). Evaluation of TMOD1 expression by primary tumoral size shows that the optimal cutoff point in the ROC curve analysis is 112.3 (AUC, 0.578; 95% CI, 0.496-0.660; sensitivity, 70.7%; specificity, 52.4%). The TMOD1 OSCCs sq-IHC scores in T1/T2 and T3/T4 range from 204.44 to 7.00 (median, 87.46) and 201.67 to 20.00 (median, 113.13), respectively. The TMOD1 protein expression in the primary OSCCs does not differ significantly (p=0.057, Student's *t*-test) between T1/T2 and T3/T4 (C). Evaluation of TMOD1 expression in primary OSCCs by histologic type shows that the optimal cutoff point in the ROC curve analysis is 119.1 (AUC, 0.665; 95% CI, 0.489-0.841; sensitivity, 68.3%; specificity, 70.0%). The TMOD1 OSCCs sq-IHC scores in well/moderately differentiated OSCCs and poorly differentiated OSCCs range from 204.44 to 7.00 (median, 100.00) and 193.17 to 34.50 (median, 138.14), respectively. The TMOD1 protein expression in the primary OSCCs does not differ significantly (p=0.073, Student's *t*-test) between

well/moderately differentiated OSCCs and poorly differentiated OSCCs (D). Evaluation of TMOD1 expression in primary OSCCs by vascular invasiveness shows that the optimal cutoff point in the ROC curve analysis is 107.0 (AUC, 0.527; 95% CI, 0.437-0.618; sensitivity, 60.4%; specificity, 60.0%). The TMOD1 OSCCs sq-IHC scores with/without vascular invasion range from 204.44 to 7.00 (median, 97.00) and 201.17 to 12.50 (median, 108.53), respectively. The TMOD1 protein expression in the primary OSCCs does not differ significantly (p=0.558, Student's *t*-test) with/without vascular invasion (E).

Figure 4. Evaluation of TMOD1 expression in primary OSCCs by RLNM. ROC curve analysis shows that the optimal cutoff point is 100.00 (AUC, 0.608; 95% CI, 0.527-0.688; sensitivity, 65.8%; specificity, 57.5%) (A). The TMOD1 OSCCs sq-IHC scores without RLNM and with RLNM range from 204.44 to 12.50 (median, 85.48) and 201.17 to 7.00 (median, 112.16), respectively (B). The TMOD1 protein expression in the primary OSCCs with RLNM is significantly (p=0.0199, Student's *t*-test) higher than those without RLNM.

Figure 5. Evaluation of TMOD1 expression in primary OSCCs in patients with 5-year survival. Using the RLNM cutoff value from the ROC curve analysis, the TMOD1 expression level is significantly (p=0.0064, log-rank test) correlated with the 5-year survival. The 5-year survival rates in the TMOD1-positive OSCCs (n=103) and the TMOD1-negative OSCCs (n=97) are 60.4% and 79.9%, respectively.

Figure 1

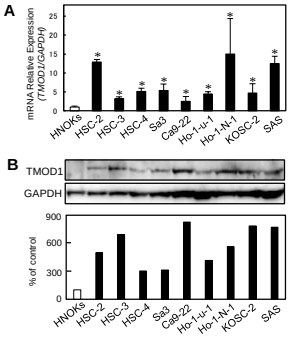
A
mRNA Relative Expression
(TMOD1/GAPDH)
25
20
15
10
5
0
HNOKs
HSC-2
HSC-3
HSC-4
Sa3
Ca9-22
Ho-1-U-1
Ho-1-N-1
KOSC-2
SAS
B
TMOD1
GAPDH
900
600
300
0
% of control
HNOKs
HSC-2
HSC-3
HSC-4
Sa3
Ca9-22
Ho-1-U-1
Ho-1-N-1
KOSC-2
SAS

Figure 2

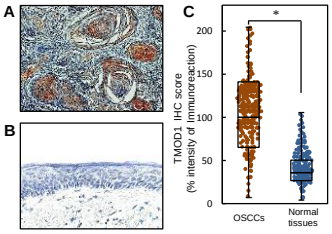
A
B
C
*
200
150
100
50
0
TMOD1 IHC score
(% intensity of immunoreaction)
OSCCs
Normal
tissues

Figure 3

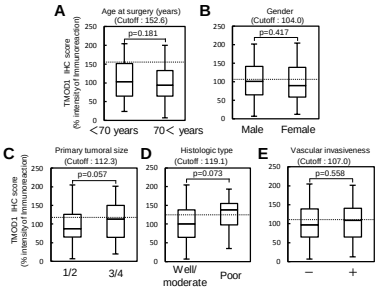
A
Age at surgery (years)
(Cutoff : 152.6)
p=0.181
TNOD1 IHC score
(% intensity of immunoreaction)
<70 years
70< years
B
Gender
(Cutoff : 104.0)
p=0.417
Male
Female
C
Primary tumoral size
(Cutoff : 112.3)
p=0.057
1/2
3/4
D
Histologic type
(Cutoff : 119.1)
p=0.073
Well/
moderate
Poor
E
Vascular invasiveness
(Cutoff : 107.0)
p=0.558
−
+

Figure 4

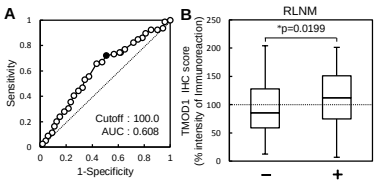
A
Sensitivity
1-Specificity
Cutoff : 100.0
AUC : 0.608
B
RLNM
*p=0.0199
TMOD1 IHC score
(% intensity of immunoreaction)
–
+

Figure 5

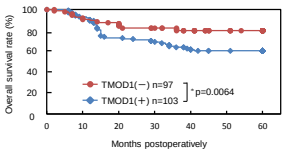
100
80
60
40
20
0
Overall survival rate (%)
0
10
20
30
40
50
60
Months postoperatively
TMOD1(−) n=97
TMOD1(+) n=103
*p=0.0064

Table 1. Clinical classification in OSCCs from 200 patients.

Variable	No. patients	(%)
Age at surgery (years)		
<70	111	55.5
≧70	89	44.5
Gender		
Male	132	66
Female	68	34
T-primary tumor		
T1+ T2	116	58
T3+ T4	84	42
N-regional lymph node		
Negative	120	60
Positive	80	40
Histopathologic type		
Well and moderately differentiated	190	95
Poorly differentiated	10	5
Vascular invasion		
Negative	149	74.5
Positive	51	25.5

Table 2. Prospective study of TMOD1 expression in primary OSCCs from 40 patients.

Relative expression	RLNM (n=40)		P value
	- (%)	+ (%)	
High TMOD1	9 (37.5%)	12 (75%)	0.027
Low TMOD1	15 (62.5%)	4 (25%)	
Total	24 (100%)	16 (100%)	

High TMOD1 expression is seen in 12 (75%) of 16 RLNM-positive patients and nine (37.5%) of 24 RLNM-negative patients. Low TMOD1 expression is seen in four (25%) of 16 RLNM-positive patients and 15 (62.5%) of 24 RLNM-negative patients.

International Journal of Oncology.　Vol 48　No 2
平成 28 年 2 月　公表済み